we observe that the bare C_9, C_{13}, and C_{17} peaks are replaced by hydrogenated product peaks which are similar both qualitatively and quantitatively to those which result from C_{11}, C_{15}, and C_{19} even though the bare peaks of the former set are at least an order of magnitude weaker than those of the latter. In fact the resulting features vary rather gradually in pattern *and* intensity across the range of odd n products. Because we cannot interpret the hydrogenated peaks for odd n, it is not clear whether we are observing parent ions. However, the smooth variation of ion intensities with n (odd) suggests that the neutral precursors are more closely related in character than the original $\Delta n = 4$ pattern implies. This suggests that the characteristic intensity pattern of the mass spectrum observed for the bare clusters in Figure 1a may be dominated by ion fragmentation and is not a true diagnostic of the neutral cluster relative abundance. The $\Delta n = 4$ effect may be due in some way to ring structures—probably of the *ions* ultimately detected.

After the work detailed here was completed the interesting experiments of Devienne and Teisseire[11] were brought to our attention. Their observations and ours are complementary as they have shown that, given carbonaceous grain (graphitic) particles, a range of interstellar species can be produced by grain bombardment with high-energy neutrals.

In the present experiments we conclude that such species can be formed more or less simultaneously with carbonaceous grains. Although the conditions in our experiments differ from those in stellar atmospheres, it is highly likely that the main features of the carbon nucleation process are similar. Therefore, we feel that these experiments demonstrate a simple way in which the long-chain cyanopolyynes observed by radioastronomy can be formed in regions where carbon is condensing, and in the absence of any alternative similarly convincing interstellar process, the results suggest a different source of these species from those heretofore considered.[12,11]

Acknowledgment. This research was supported by the N.S.F. and the Robert A. Welch Foundation and used a laser and molecular beam apparatus supported by the U.S. Army Research Office and U.S. Department of Energy. H.W.K. acknowledges the S.E.R.C. (U.K.) for financial support. We thank the referees for helpful comments and in particular for bringing the work of Devienne and Teisseire to our attention.

Is Delocalization a Driving Force in Chemistry? Benzene, Allyl Radical, Cyclobutadiene, and Their Isoelectronic Species

Sason S. Shaik,*[1a] Philippe C. Hiberty,*[1b] Jean-Michel Lefour,[1b] and Gilles Ohanessian[1b]

Contribution from the Department of Chemistry, Ben Gurion University, Beer Sheva 84105, Israel, and Laboratoire de Chimie Théorique,† Université de Paris-Sud, 91405 Orsay, France.
Received May 6, 1986

Abstract: The VB correlation diagram model (Figure 1) is used to answer the title question. It is shown that *only atoms that form weak two-electron bonds with low triplet excitation energies may generate delocalized species that are stable toward a localizing distortion.* Electronic delocalization is, then, seldom expected to be a significant driving force in chemistry. By this principle, the π-components of delocalized species, like C_6H_6 and C_3H_5, are predicted to be distortive electronic systems that are trapped, within "rigidly" symmetric σ-frames, and are thereby delocalized despite their opposite inherent tendency. The predictions are examined by means of ab initio investigations at the levels of STO-3G, 6-31G, and 6-311G with extensive correlation (CI) calculations (up to 6×10^6 determinants). σ–π energy partitions show that the π-components of C_6H_6 and C_3H_5 are indeed distortive much like the π-electrons of C_4H_4, and all the π-components resemble, in turn, their isoelectronic H_n (n = 3, 4, 6) species in the common reluctance to adopt geometries that lead to electronic delocalization. *Electronic delocalization* in C_3H_5 and C_6H_6 *turns out to be a byproduct of the σ-imposed geometric symmetry and not a driving force by itself.* The π-distortive propensities are shown to coexist harmoniously with the thermochemical stability of benzene and the rotational barrier of allyl radical. Further application of the model shows that π-delocalization, per se, is seldom expected to be a driving force in organic molecules containing C, N, and O. In this manner the delocalization problem is unified and shown *not* to be merely a matter of electron count and mode of delocalization.

In recent communications,[2] ab initio computational evidence has been provided that the π-electrons of allyl radical (**1**) and benzene (**2**) prefer to distort to their localized π-components, much like the π-electrons of singlet cyclobutadiene (**3**). These distortive

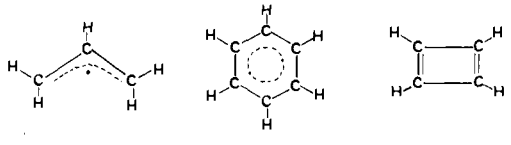

1 2 3 SINGLET

propensities in **1** and **2** are, however, quenched by the σ-frames that strongly prefer regular geometries with uniform C–C bond lengths. Consequently, π-electronic delocalization in **1** and **2** turns out to be a byproduct of a geometric constraint and occurs despite the opposite inherent tendency of the π-electrons. This result touches a key question of chemical epistemology: is electronic delocalization a driving force of stability and geometric shape? Our preliminary computational data[2] show that, in organic species, π-delocalization is not such a driving force but rather a byproduct phenomenon.

The credibility of this conclusion must be established now by a two-pronged examination. Firstly, it must be shown that it is not a computational artifact but rather a chemical trend that emerges from the broader context of chemistry. Secondly, the

† Associated with the CNRS, UA 506.

(1) (a) Ben Gurion University. (b) Laboratoire de Chimie Théorique (associated with the CNRS, UA 506).

(2) (a) Shaik, S. S.; Hiberty, P. C.; Ohanessian, G.; Lefour, J. M. *Nouv. J. Chim.* **1985**, *9*, 385. (b) Hiberty, P. C.; Shaik, S. S.; Lefour, J. M.; Ohanessian, G. *J. Org. Chem.* **1985**, *50*, 4657.

0002-7863/87/1509-0363$01.50/0

conclusion must be harmonized with various properties, such as the special thermochemical stability of benzene (**2**), the substantial rotational barrier of allyl radical (**1**), and so on.

The broader context of the delocalization problem is projected through the trends revealed by the series of X_n (n = 3, 6, 4) species that are *isoelectronic* and *isostructural* to the π-components of **1–3**. Thus, the hexagonal structures of H_6, Cl_6, Li_6, etc., form an isoelectronic series to the π-component of benzene, with a distortive behavior that ranges between the extremes **4** and **5**.

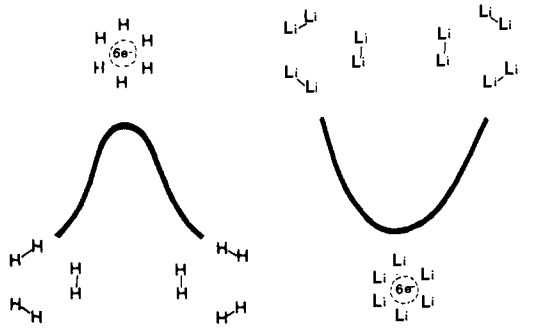

4 **5**

Clearly then, despite the aromatic stabilization that is available to all the hexagonal species, H_6, at one extreme, is unstable toward a distortion[3] to three localized components ($3H_2$), while hexagonal Li_6, at the other extreme (**5**), is stable toward the same localizing distortion.[4]

This spectrum recurs in the X_3 series (**6**)[5] and even in the antiaromatic series of X_4 squares (**7**).[6] Thus in each case, one extreme is defined by the delocalized H_n species that is unstable toward a localizing distortion (e.g., $H_3^{\bullet} \rightarrow H_2 + H^{\bullet}$),[5a-d] while the other extreme is defined by the Li_n species that is stable toward the same distortion (e.g., square $Li_4 \rightarrow 2Li_2$).[6c-f]

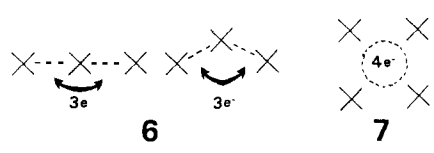

6 **7**

It is apparent then that the importance of delocalization is dependent upon the nature of the atom X and is not merely a topological matter of electron count. Understanding this dependence is, therefore, vital for ascertaining the role of π-electronic delocalization in organic species. In this manner, the π-components of **1–3** can be placed, in between the extremes, in their respective isoelectronic series. The actual propensity of the π-electrons would then be attached to some chemical property of the atom C, and the computational test would serve a conceptual purpose.

The outline of the paper follows from the above discussion. Models for predicting trends, in delocalized X_n series, have been developed before,[7,8] and section I briefly describes one of these models that is based on valence bond (VB) correlation diagrams.[7] The model is then utilized to show that the π-components of **1–3** resemble their isoelectronic H_n (n = 3, 6, 4) species in the common tendency to undergo localizing distortions.[9]

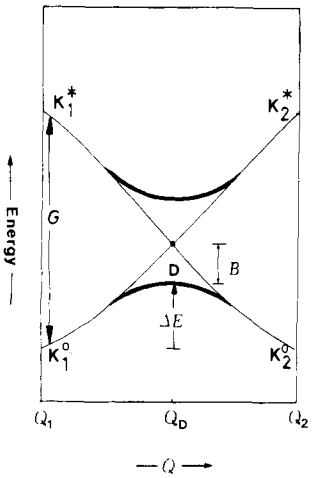

Figure 1. A correlation diagram for interconversion of two mirror-image Kekulé structures (K_1^0 and K_2^0) through the delocalized species (D), along the transformation coordinate Q; Q_1, Q_2, and Q_D signify respectively optimum geometries of the Kekulé structures and the delocalized species. Avoided crossing is shown by heavy lines and corresponds, for illustrative purposes, to a distortive **D** that is less stable than K_1^0 and K_2^0 by ΔE. This diagram applies also to the π-electrons of conjugated systems, e.g., C_4H_4, C_6H_6, C_3H_5 (σ-electrons are removed).

Section II delineates, in more details than are present in the communications,[2] various methodologies of σ–π energy partitioning within the ab initio technique. These methods are designed to test the predictions of the qualitative model. By use of the prototypical species, **1–3**, it is shown that π-delocalization is not a driving force in organic chemistry, and all the π-components indeed possess distortive propensities that are, sometimes, realized (e.g., in **3**) and, otherwise, latent (e.g., in **1** and **2**).

Subsequent sections are devoted to showing (a) why the π-component of allyl radical (**1**) can be distortive, while at the same time be exhibitive of a rotational barrier, and (b) how the π-distortive propensity can exist in benzene, which is known to possess a substantial thermochemical "resonance energy". An analysis of the elusive species N_6 (hexaazabenzene)[10] completes the cycle of topics and is presented to demonstrate the predictive power of the model and its conceptual insight into the leading question: is delocalization a driving force in chemistry?

I. VB State Correlation Diagram Model[7]

Consider two different geometries of the target species X_n (n = 3, 4, 6). One geometry allows electronic delocalization and consists of symmetric linear or bent X_3 (**6**), square X_4 (**7**), and hexagonal X_6. The other geometry prohibits electronic delocalization and consists of the localized components of X_3, X_4, and X_6. An example of the latter geometry for the X_6 series is shown in **8a,b**, where the short X–X distance is the equilibrium bond

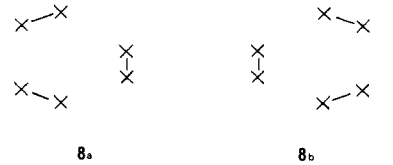

8a **8b**

length of the dimer X_2, and the other distance is infinite. These

(3) (a) Dixon, D. A.; Stevens, R. M.; Herschbach, D. R. *Faraday Discuss. Chem. Soc.* **1977**, *62*, 110. (b) Haddon, R. C.; Raghavachari, K.; Whangbo, M. H. *J. Am. Chem. Soc.* **1984**, *106*, 5364. (c) Ichikawa, H. *J. Am. Chem. Soc.* **1984**, *106*, 6249; **1983**, *105*, 7467.

(4) (a) Reference 3a. (b) Plavsic, D.; Koutecky, J.; Pacchioni, G.; Bonacic-Koutecky, V. *J. Phys. Chem.* **1983**, *87*, 1096. (c) Pickup, B. T. *Proc. R. Soc. London, A* **1973**, *333*, 69. (d) Shaik, S. S.; Hiberty, P. C. *J. Am. Chem. Soc.* **1985**, *107*, 3089.

(5) (a) Liu, B. *J. Chem. Phys.* **1973**, *58*, 1925. (b) Reference 4d. (c) Reference 3a. (d) Parr, C. A.; Truhlar, D. G. *J. Phys. Chem.* **1971**, *75*, 1844. (e) Kendrick, J.; Hillier, I. H. *Mol. Phys.* **1977**, *33*, 635. (f) Reference 2a. (g) Beckmann, H. O. *Chem. Phys. Lett.* **1982**, *93*, 240. (h) Yardley, R. N.; Balint-Kurti, G. G. *Chem. Phys.* **1976**, *16*, 287. (i) Inglesfield, J. E. *J. Chem. Phys.* **1977**, *67*, 505. (j) Gerber, W. H.; Schumacher, E. *J. Chem. Phys.* **1978**, *69*, 1692. (k) Companion, A. L. *Chem. Phys. Lett.* **1978**, *56*, 500. (l) Wu, C. H. *J. Chem. Phys.* **1976**, *65*, 3181. (m) Lindsay, D. M.; Herschbach, D. R.; Kwiram, A. L. *Mol. Phys.* **1976**, *32*, 1199.

(6) (a) Silver, D. M.; Stevens, R. M. *J. Chem. Phys.* **1973**, *59*, 3378. (b) Reference 3a,b. (c) Wu, C. H. *J. Phys. Chem.* **1983**, *87*, 1534. (d) Beckmann, H. O.; Koutecky, J.; Bonacic-Koutecky, V. *J. Chem. Phys.* **1980**, *73*, 5182. (e) Reference 5k. (f) Malrieu, J. P.; Maynau, D.; Daudey, J. P. *Phys. Rev. B: Condens. Matter* **1984**, *30*, 1817.

(7) (a) Shaik, S. S.; Bar, R. *Nouv. J. Chim.* **1984**, *8*, 411. (b) Reference 4d.

(8) Epiotis, N. D. *Nouv. J. Chim.* **1984**, *8*, 11. Epiotis, N. D. *Lect. Notes Chem.* **1983**, *34*, 358–371. Epiotis, N. D. *Pure Appl. Chem.* **1983**, *55*, 229.

(9) See the debate in ref 3b and 3c.

(10) Saxe, P.; Schaefer, H. F., III. *J. Am. Chem. Soc.* **1983**, *105*, 1760.

distorted and localized forms, for each X_n, will be termed hereafter *Kekulēan structures*. Likewise, the associated geometric distortion, of the regular species to the localized components, will be referred to as a *localizing* distortion.

Figure 1 describes, for each X_n, the general relationship between the localized Kekulēan structures (K_1^0 and K_2^0) and the delocalized species (D).[7] The delocalized species is generated through the avoided crossing of two energy curves, along a coordinate that interchanges the geometries of the two Kekulēan structures. The curves are anchored, at each end, at the ground state and a specific excited configuration of the Kekulēan structures (e.g., K_1^0 and K_1^*).

The specific excited configurations are those that prepare their ground Kekulē forms for the requisite bond shift. For example, K_1^* is obtained, from K_1^0, by a specific electronic promotion that generates the electron-pairing scheme of K_2^0. Thus, K_1^* possesses the geometry of K_1^0 and the electron-pairing scheme of K_2^0, and hence, K_1^* will correlate with K_2^0 along the interchange coordinate ($Q_1 \rightarrow Q_2$). Symmetric arguments apply to the $K_2^* \rightarrow K_1^0$ correlation curve.

The two energy curves intersect at the regular geometry (uniform X–X distances) and avoid the crossing by their mutual mixing. Contrary to MO correlation diagrams where avoided crossing is dictated by orbital symmetry, in VB correlation diagrams all cases uniformly exhibit avoided crossings. The avoided crossing, which is shown by heavy lines in Figure 1, generates the delocalized state (D) that is stabilized, relative to the crossing point, by *the resonance interaction B*.

The energy of the delocalized species (D) relative to the localized forms (K_1^0 and K_2^0) is determined by two opposing factors: the energy gap G and the resonance interaction B. Equation 1 expresses this balance in a semiquantitative form that derives from Figure 1.

$$\Delta E(K_i^0 \rightarrow D) = fG - B \quad (f = \text{a fraction} < 1) \qquad (1)$$

The first term fG measures the energy—invested to reach the cross point—as a fraction (f) of the energy gap between the curves. Thus, the factor that opposes delocalization is associated with the energy, G, required to reorganize the electrons of a Kekulē form and electronically prepare it for bond shift, at a frozen geometry. The larger the G factor the more reorganization energy is required to reach the crossing point. Once electronic reorganization takes place and the energy equality of two electron-pairing schemes is established at the crossing point, energy is then gained by delocalization, and this is the resonance interaction B that appears in eq 1. The value of B is typical of the isoelectronic series and reflects the topology effects that depend on the number of electrons in a particular mode of delocalization. This is the physical essence of the model.

To make predictions, the balance between G and B must be specified for each X_n species. In previous publications[2a,7] it has been concluded that G is the dominant factor in *each* isoelectronic series.[11] Accordingly, an ensemble of *delocalized* isoelectronic species is expected to generate a spectrum between the two extremes, described in **9a** vs. **9b** in a diagrammatic form. The

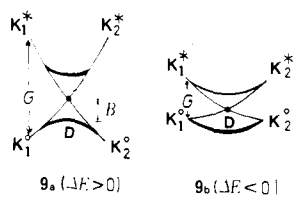

9a ($\Delta E > 0$) **9b** ($\Delta E < 0$)

stability and distortive properties of the delocalized species will be dominated then by the value of G.[11] Cases possessing large gaps will generate unstable and distortive delocalized states, as in **9a**, while cases with small gaps will feature stable, nondistortive delocalized states, as in **9b**.

Physically, the difference between these extremes derives from the reorganization energy that is required to force the two Kekulē forms into resonance (energy equality at the crossing point). When the reorganization energy is large, it overwhelms the resonance interaction (B), and electronic delocalization is then disfavored, as in **9a**. On the contrary, small reorganization energy can be overcompensated by the resonance interaction, and electronic delocalization then becomes a driving force, as in **9b**. It should be emphasized that the model does not distinguish between distortive delocalized species which differ in the modality of their potential energy curve, that is, a unimodal potential like **9a** vs. a double minimum with D occupying the top of a barrier.

To apply the predictions, an explicit expression for G is required for each of the X_n (n = 3, 4, 6) series. Consider, for example, the X_4 isoelectronic series. K_1^0 and K_2^0 are shown in **10a** and **10b**,

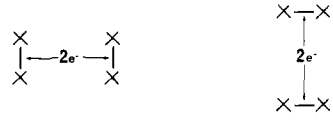

10a (K_1^0) **10b** (K_2^0)

where the short X–X linkages are the usual electron-pair bonds, each possessing a spin-couple.[4d] The excited configurations K_1^* is the one that possesses the electron-pairing scheme of K_2^0 and is shown schematically in **11**, where the circles symbolize electrons

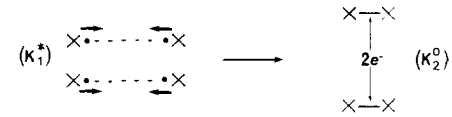

11

and the arrows represent spins. As can be seen, the electrons in K_1^* are spin-coupled across the long linkages and are unpaired across the short linkages. K_1^* is then the electronic image of K_2^0, and the correlation $K_1^* \rightarrow K_2^0$ will be established along the coordinate that interchanges the X–X distances. The same arguments can serve to generate the other excited configuration K_2^*.

The electronic relationship between K_1^* and K_1^0 (also K_2^* and K_2^0) determines the energy gap in the correlation diagram. This relationship is seen to be very simple: each one of the electron-pair bonds of K_1^0 (**10a**) is unpaired in K_1^* by a local excitation that is best approximated by a triplet, and the electrons are then spin-coupled, in pairs, across the long linkages (see Appendix 1 for derivations). The energy gap in the correlation diagram is given then by eq 2, where $\Delta E_{ST}(X_2)$ is the triplet excitation energy of the localized electron-pair bond in the X_2 molecule.

$$G(X_4) \cong {}^3/_2 \Delta E_{ST}(X_2) \qquad (2)$$

The energy gaps for the other series, X_3 and X_6, can be obtained easily by using the foregoing electron reorganization relationship between the ground and excited anchor points (K_i^* and K_i^0; i = 1, 2). To generate K_i^* from K_i^0 one must initially unpair every localized X–X electron-pair bond and then spin-couple, in pairs, all the electrons across the long linkages.[7] The energy gaps for the X_3[2a] and X_6 series become then n-fold the quantity ${}^3/_4 \Delta E_{ST}(X_2)$, where n is the number of localized bonds that have to be promoted to triplets. These approximate expressions are given in eq 3a and 3b, and more accurate ones are derived in Appendix 1.

$$G(X_3) \cong {}^3/_4 \Delta E_{ST}(X_2) \qquad (3a)$$

$$G(X_6) \cong {}^9/_4 \Delta E_{ST}(X_2) \qquad (3b)$$

The energy gap G, which opposes delocalization in X_3, X_4, and X_6, is seen to be proportional, in each case, to the triplet excitation

(11) This does not mean that B and f are constants in the series. It only means that the variation of G in a series is the dominant factor. To see that, consider the B (QMRE) values in Table VI for H_6 and C_6H_6. The B value of the former is ~20 kcal/mol larger, while the corresponding G values vary by 329 kcal/mol (see Table I and eq 3b). The relative invariance of B has been deduced in other problems that obey the VB correlation diagram; see: (a) Mitchell, D. J.; Schlegel, H. B.; Shaik, S. S.; Wolfe, S. *Can. J. Chem.* **1985**, *63*, 1642. (b) Shaik, S. S. *Prog. Phys. Org. Chem.* **1985**, *15*, 197.

Table I. Distortive Properties of Delocalized X_n Species

			ΔE, kcal/mol[a]								
			X_6			X_3			X_4		
(X)[o]	$\Delta E_{ST}(X_2)$[b]	$D_e(X_2)$[c]	I[d]	II[e]	III[g]	I[h]	II[j]	III[k]	I[l]	II[m]	III[n]
(1) H	246	106	+74.4	+86.0		+9.8	+12.4	+9.8	+147	+63	
(2) Cl		58		+8.1	>0		≥0	1, ∼0			≥+30
(3) Li	32	25	−10.9	−32.9		−5.3	−9.8	−16 ± 5	−2.0	−20.1	−27
						(−9.2)[i]	(−10.1)[i]				
(4) Na	25	18		−24[f]		−5.5	−7.8		+1.0	−15.7	
						(−8.4)[i]	(−7.8)[i]				
(5) C[p]	100	∼60									

[a] $\Delta E > 0$ means that the delocalized species is unstable toward a localizing distortion and vice versa. [b] ΔE_{ST} in kcal/mol, respectively, from ref 13a–d. [c] D_e is the bond energy in kcal/mol, respectively, from ref 14a–e. [d] Ab initio results, respectively, from ref 3a and 4b. [e] DIM results, respectively, from ref 3a, 15, and 16. [f] Estimated from ref 17. [g] Experimental values from ref 18. [h] Ab initio results, respectively, from ref 5a, 5e, and 19. [i] The values out of parentheses are for linear X_3, while the parenthetical values are for bent X_3. [j] DIM results, respectively, from ref 3a, 20, 5k, and 6f. [k] Experimental values, respectively, from ref 5d, 21, and 5l. [l] Ab initio results, respectively, from ref 6a, 6d, 6d. [m] DIM results, respectively, from ref 3a, 5k, and 6f. [n] Experimental results, respectively, from ref 3a (18) and 6c. [o] Entry numbers are in parentheses.

energy of the localized bonds. It follows then that the *isoelectronic spectrum* described by **9a** → **9b** will be dominated by $\Delta E_{ST}(X_2)$.[11] Large $\Delta E_{ST}(X_2)$ values are expected to generate unstable delocalized X_n ($n = 3, 4, 6$) species that possess a distortive tendency, while small $\Delta E_{ST}(X_2)$ values are expected to lead to stable and nondistortive delocalized species.

Generally, the triplet excitation of a bond is related to its strength,[7a] so that large $\Delta E_{ST}(X_2)$ values are associated with strong bonds and vice versa.[12] It follows then that the stability of the delocalized species toward a localizing distortion will generally be inversely proportional to the X–X bond strength.[12] This relationship leads to the following simple conclusion: *electronic delocalization is expected to be an important driving force only for atoms X that form weak bonds.*[7,8] Weak bonds are associated with small reorganization energies that accompany enforcement of the Kekulé forms into resonance. The resonance interaction can overcompensate for such small reorganization energies, and thereby electronic delocalization is favored.

The manifestations of this qualitative conclusion are shown in Table I for hexagonal X_6, linear or bent X_3, and square X_4 species.[12-21] Each series exhibits a spectrum, of the type **9a** → **9b**, that depends on the triplet excitation and the bond strength of the localized X–X dimer. It appears that the propensity of a system to be delocalized is indeed restrained by the large reorganization energy that is associated with strong X–X bonds. Delocalization becomes a driving force ($\Delta E < 0$) only for very weak bonds. Many other data are in line with this general statement.[22]

With a rational physical modeling of the problem it is appropriate to ask now the more complicated questions. Is π-delocalization in benzene and allyl radical a driving force on its own? Would the π-components of these species be delocalized were they not buttressed by the σ-frames? The triplet excitation energy of a π_{CC}-bond and its strength are given in entry 5 of Table I. These values are substantial and much higher than those that render delocalization a driving force. The margin of confidence is wide enough to place the π-components in the unstable branch of each isoelectronic spectrum: in between the corresponding H_n and Cl_n species.

The resemblance of the bond strength parameters of π-components and Cl_n species allows us to specify the predictions. Thus, the π-component of allyl radical should be slightly distortive or indifferent to distortion ($\Delta E \cong 0$). On the other hand, the π-component of benzene should possess a clear propensity to distort. In each case, π-electronic delocalization must then be a byproduct phenomenon of the geometric constraints exerted by the σ-frame. The π-components of C_6H_6, C_3H_5, and C_4H_4, possess then the same qualitative behavior and wish to distort to their localized components. It remains now to quantify these distortive propensities and harmonize them with other known properties of these systems.

Before doing that it is appropriate to put the present model into context with previous and recent work. The idea that the π-component of benzene is distortive dates back to 1959 when Longuet-Higgins and Salem,[23a,b] following Labhart[23c] and Ooshika,[23d] proposed, on the basis of a variable-β-Hückel treatment and pseudo-Jahn–Teller-effect arguments, that the tendency of a $(4n + 2)$ π-electronic system to distort "exists alread in benzene".[23b] Similar arguments, coupled with an analysis of the experimental B_{2u} vibration, were later on used by Berry[24] to derive the same conclusion. This distortive propensity recurs also in the semiempirical calculations of Paldus et al.[25] and have been deduced also by Heilbronner.[26]

The distortive properties of the π-component of allyl radical

(12) Usually, $\Delta E_{ST} \cong 2D_e$. F_2 is an exception. Its bond energy is only about 38 kcal/mol, this being due to the strong repulsion between electron pairs, while the triplet excitation is large: 161 kcal/mol. See: Cartwright, D. C.; Hay, P. J. *J. Chem. Phys.* **1979**, *70*, 3191. It is always advisable to use the more reliable criterion of the triplet excitation energy.

(13) (a) Kolos, W.; Wolniewicz, L. *J. Chem. Phys.* **1965**, *43*, 2429. (b) Konowalow, D. D.; Olson, M. L. *J. Chem. Phys.* **1979**, *71*, 450. Konowalow, D. D.; Olson, M. L. *Chem. Phys.* **1977**, *21*, 393. (c) Konowalow, D. D.; Rosenkrantz, M. E.; Olson, M. L. *J. Chem. Phys.* **1980**, *72*, 2612. (d) Jordan, K. D.; Burrow, P. D. *J. Am. Chem. Soc.* **1980**, *102*, 6882.

(14) (a) Reference 3a. (b) Kerr, J. A.; Parsonage, M. J.; Trotman-Dickenson, A. F. *Handbook of Chemistry and Physics*; CRC: Cleveland, 1976; pp F204. (c) Reference 6c. (d) Reference 13c. (e) Walsh, R. *Acc. Chem. Res.* **1981**, *14*, 246. Benson, S. W. *J. Chem. Educ.* **1965**, *42*, 502.

(15) Reference 3a and: Thompson, D. L.; Suzukawa, H. H., Jr. *J. Am. Chem. Soc.* **1977**, *99*, 3614.

(16) References 3a and 4c.

(17) Gelb, A.; Jordan, K. D.; Silbey, R. *Chem. Phys. Lett.* **1975**, *9*, 175.

(18) Estimated from data in: Dixon, D. A.; Herschbach, D. R. *J. Am. Chem. Soc.* **1975**, *97*, 6268.

(19) Martin, R. L.; Davidson, E. R. *Mol. Phys.* **1978**, *35*, 1713.

(20) Various Cl_3 DIM and LEPS computations provide a range of ΔE values from −2 kcal/mol to ∼5 kcal/mol. See: (a) Reference 5d. (b) Sato, S. *J. Chem. Phys.* **1965**, *23*, 2465. (c) Koshi, M.; Ito, H.; Matsui, H. *Chem. Phys. Lett.* **1983**, *103*, 180.

(21) Cl_3 is found experimentally to be weakly bound and to possess a distorted structure with slight bond alternation. See: Lee, Y. T.; Lebreton, P. R.; McDonald, J. D.; Herschbach, D. R. *J. Chem. Phys.* **1969**, *51*, 455. Nelson, L. Y.; Pimentel, G. C. *J. Chem. Phys.* **1967**, *47*, 3671.

(22) (a) K_3 seems to be bound in accord with the small $\Delta E_{ST}(K_2)$ value. See ref 5m. (b) The Br_3 and I_3 species with intermediate bond strength are either bound or possess small tendency to distort (i.e., X_3 is a transition state). See ref 21 and: Bunker, D. L.; Davidson, N. *J. Am. Chem. Soc.* **1958**, *80*, 5090. Noyes, R. M.; Zimmerman, J. *J. Chem. Phys.* **1950**, *18*, 656. Noyes, R. M. *J. Am. Chem. Soc.* **1966**, *88*, 4311. Blake, J. A.; Burns, G. *J. Chem. Phys.* **1971**, *54*, 1480. (c) Hexagonal X_6 species involving X = Br and/or I were inferred to be only slightly (1–3 kcal/mol) higher in energy than the localized dimers. See ref 18 and: Schweitzer, P.; Noyes, R. M. *J. Am. Chem. Soc.* **1971**, *93*, 3561.

(23) (a) Longuet-Higgins, H. C.; Salem, L. *Proc. R. Soc. London, A* **1959**, *251*, 172. (b) Salem, L. *The Molecular Orbital Theory of Conjugated Systems*; W. A. Benjamin: Reading, MA, 1972; pp 103–106, 494–505. (c) Labhart, H. *J. Chem. Phys.* **1957**, *27*, 957. (d) Ooshika, Y. *J. Phys. Soc. Jpn.* **1957**, *12*, 1238, 1246.

(24) Berry, R. S. *J. Chem. Phys.* **1961**, *35*, 29, 2253.

(25) Paldus, J.; Chin, E. *Int. J. Quantum Chem.* **1983**, *24*, 373.

(26) Heilbronner, E., private communication. See also: Heilbronner, E.; Binsch, G.; Murrell, J. N. *Mol. Phys.* **1966**, *11*, 305. Heilbronner, E.; Binsch, G.; Murrell, J. N. *Tetrahedron* **1968**, *24*, 1215.

were extensively discussed by several groups in the context of the doublet instability of the restricted Hartree–Fock (RHF) wave function.[27] More recently, the pseudo-Jahn–Teller model[28] was utilized to discuss the distortive properties in allylic type systems such as the formyloxyl radical.

A common feature of all the early models, such as the pseudo-Jahn–Teller effect and the variable-β-Hückel treatment, is that they predict that in principle all the isoelectronic species, of the type X_3 and X_6, should possess a distortive tendency.[29] On the other hand, the VB models of Epiotis[8] and Malrieu[30] and the present treatment[7] project the spectrum of behavior (**9a** → **9b**) and provide a rational physical reason for the distortive propensity of π-components. At any rate, all the models are essentially qualitative, and the specific prediction must ultimately be tested by means of ab initio computations at the highest possible level. Such a test would be an initial answer to the leading question: is electronic delocalization a driving force?

II. Computational Tests for C_6H_6, C_3H_5, and C_4H_4

1. Methods and Strategy. The ab initio SCF calculations reported here were performed with three different Gaussian-contracted basis sets: STO-3G,[31] 6-31G,[32] and 6-311G.[33] The latter is specifically designed for post-SCF calculations. The closed-shell species were calculated with the closed-shell SCF formalism, while open-shell species were computed with the RHF method.[34] The singlet cyclobutadiene which is a diradical was computed with the restricted open-shell method of Davidson.[35] All calculations were performed with the MONSTERGAUSS series of programs.[36] Monoelectronic and bielectronic integrals which are required for the $\sigma-\pi$ energy partition via eq 5 (see later) are extracted directly from the program's subroutines.

Whenever specified, the effect of electron correlation was studied by using the CIPSI algorithm.[37] In this method, a variational zero-order wave function is constructed by an iterative selection of the most important determinants. All single and double substitutions derived from each of the determinants in the zero-order wave function are generated and taken into account through second-order Møller–Plesset perturbation theory. Determinants having a coefficient larger than a given threshold in the first-order wave function are then included in the zero-order one, and the perturbation calculation is repeated. The selected threshold defining the zero-order wave function is thus gradually lowered until the numerical value (for example, the relative energy that one wants to estimate) is converging. As orders of magnitude, the most sophisticated calculations for allyl radical, with the 6-311G basis, include about 6×10^6 determinants with a threshold of 0.015. For larger molecules, the most sophisticated calculations, at the 6-31G level, are restricted to π-space CI with thresholds of 0.010 for benzene and cyclobutadiene. At the STO-3G level, the π-space CI is always complete.

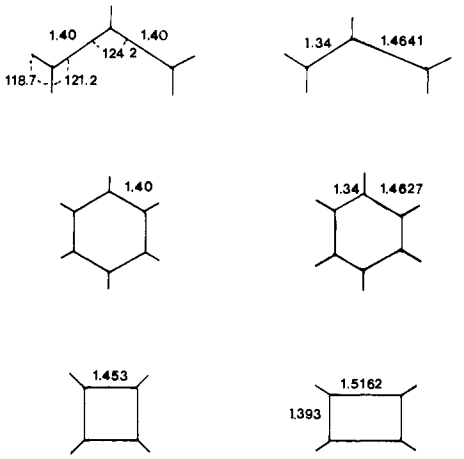

Figure 2. Symmetric and distorted geometries for allyl radical, benzene, and singlet cyclobutadiene. The distortions keep constant nuclear repulsions between carbons. Bond angles are the same for distorted and undistorted structures.

The strategy is as follows. The symmetric structures are distorted partway toward their localized components as illustrated in Figure 2. Then the total energy change that accompanies the distortion is partitioned into its π- and σ-contributions to verify or falsify the predicted π-distortive propensity.

The selected distortion is very crucial, because a wrong distortion will lead to a wrong conclusion. Consider, for example, the hexagonal H_6 structure. This structure is a transition state for the exchange reaction of three H_2 molecules.[3a] The transition state possesses *only one mode* with a negative force constant. This is the B_{2u} mode[3a] along which the total energy is lowered. All the other distortions possess positive force constants. Thus, if we were to probe the distortive properties of H_6 along a mode that is not B_{2u}, the energy would rise upon distortion and an erroneous conclusion would result: that hexagonal H_6 is a stable structure. In complete analogy, if indeed the π-components of benzene and allyl radical are distortive, then this property must be searched along the B_{2u} and B_2 modes, respectively.

Another point of concern is that if the distortion involves significant changes in the nuclear repulsion, then the $\sigma-\pi$ energy partition would not be meaningful (see later discussion). The distortions in Figure 2 are selected so as to meet simultaneously the two requirements. Alternately compressing one bond by 0.06 Å and stretching the other by nearly the same amount achieves near identity of the distortions with the corresponding B_{2u} and B_2 vibrational modes of benzene and allyl. The small differences in the third figure of the stretched bonds (1.4627 Å; 1.4641 Å instead of 1.4600 Å) achieves the second requirement of constancy in the nuclear repulsion (see later discussion).[38] The same strategy was applied to singlet cyclobutadiene starting from the symmetric square geometry, reported by Borden et al.[39,40]

2. Distortive Properties of π-Systems. Allyl Radical.[2a] It is known that allyl radical resists the localizing distortion[41] in **12**, that is, the total distortion energy, $\Delta E^{\pi,\sigma}_{dis}$, is positive. Under constant nuclear repulsion, this distortion energy can be conceptualized as the outcome of σ- and π-electronic driving forces,

(27) (a) Paldus, J.; Veillard, A. *Mol. Phys.* **1978**, *35*, 445. (b) Kikuchi, O. *Chem. Phys. Lett.* **1980**, *72*, 487. (c) Takada, T.; Dupuis, M. *J. Am. Chem. Soc.* **1983**, *105*, 1713. (d) McKelvey, J. M.; Berthier, G. *Chem. Phys. Lett.* **1976**, *41*, 476.

(28) (a) Feller, D.; Davidson, E. R.; Borden, W. T. *J. Am. Chem. Soc.* **1984**, *106*, 2513. (b) The distortive propensity in allyl was analyzed by using ab initio results (3-21G/MCSCF). Unpublished results: Borden, W. T. Presented at the 185th National Meeting of the American Chemical Society, Seattle, WA, March 1983.

(29) (a) This is indeed what is found by extended Hückel computations of many delocalized species, including those that are not really distortive (e.g., $C_3H_5^+$): Shaik, S. S., unpublished results. (b) Using orbital or state energy gap criteria, the pseudo-Jahn–Teller argument predicts Li_n to be more distortive than H_n and, in general, all X_n to have some distortive propensity.

(30) Malrieu, J. P. *Nouv. J. Chim.* **1986**, *10*, 61.

(31) Hehre, W. J.; Stewart, R. F.; Pople, J. A. *J. Chem. Phys.* **1969**, *51*, 2657.

(32) (a) Francl, M. M.; Pietro, W. J.; Hehre, W. J.; Binkley, J. S.; Gordon, M. S.; DeFrees, D. J.; Pople, J. A. *J. Chem. Phys.* **1982**, *77*, 3654. (b) Gordon, M. S.; Binkley, J. S.; Pople, J. A.; Pietro, W. J. *J. Am. Chem. Soc.* **1982**, *104*, 2797. (c) Pietro, W. J.; Francl, M. M.; Hehre, W. J.; DeFrees, D. J.; Pople, J. A.; Binkley, J. S. *J. Am. Chem. Soc.* **1982**, *104*, 5039.

(33) Krishnan, R.; Binkley, J. S.; Seeger, R.; Pople, J. A. *J. Chem. Phys.* **1980**, *72*, 650.

(34) Hurley, A. C. *Introduction to the Electron Theory of Small Molecules*; Academic: New York, 1976.

(35) Davidson, E. R. *Chem. Phys. Lett.* **1973**, *21*, 565.

(36) Peterson, M.; Poirier, R. MONSTERGAUSS; Department of Chemistry, University of Toronto, Ontario, Canada, 1981.

(37) Huron, B.; Malrieu, J. P.; Rancurel, P. *J. Chem. Phys.* **1973**, *58*, 5745.

(38) This distortion has been examined for hexagonal H_6 and leads to the right conclusion that the species is distortive. The changes in the third figure are too small here, and the distortion is B_{2u} for all practical purposes.

(39) Borden, W. T.; Davidson, E. R.; Hart, P. *J. Am. Chem. Soc.* **1978**, *100*, 388.

(40) The geometries of allyl and benzene are optimized at the level of full-space π-CI with the STO-3G basis set. The optimized geometries are identical with those reported in: (a) Bernardi, F.; Robb, M. A.; Schlegel, H. B.; Tonachini, G. *J. Am. Chem. Soc.* **1984**, *106*, 1198. (b) Tomagawa, K.; Ijimra, T.; Kimura, M. *J. Mol. Struct.* **1976**, *30*, 243.

(41) (a) Fessenden, R. W.; Schuler, R. H. *J. Chem. Phys.* **1963**, *39*, 2147. (b) Reference 27c.

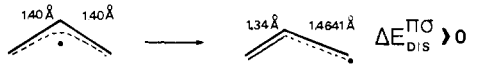

12

as expressed in eq 4. Each one of these driving forces may cause

$$\Delta E_{dis}^{\pi,\sigma} = \Delta E_{dis}^{\sigma} + \Delta E_{dis}^{\pi} \quad (>0) \tag{4}$$

$\Delta E_{dis}^{\pi\sigma}$ to be positive. A priori, the reason why allyl radical resists the localizing distortion is not known, and the root cause must be searched by determining ΔE_{dis}^{π} and ΔE_{dis}^{σ} separately.

The ΔE_{dis}^{σ} value can be derived by performing the distortion on a state of allyl in which π-delocalization is "turned off". The quadruplet $^4A_2$ state of allyl radical (**13**) is such a state because

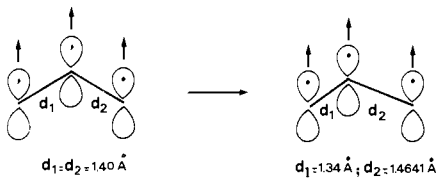

13

its π-electrons that possess identical spins do not form bonds and are energetically almost indifferent to the distortion. Indeed, this distortion consists of the shortening of one local triplet and the lengthening of the other. The bond length–bond energy dependence of the triplet state of ethylene is nearly linear in this range of bond lengths, and hence, the shortening and lengthening cause jointly a negligible net energetic effect.

The π-insensitivity to the distortion in **13** becomes evident by calculating the distortion energy of quadruplet H_3 that is isoelectronic to the π-component of quadruplet allyl radical. This distortion energy is illustrated in **14** and is found to be marginally

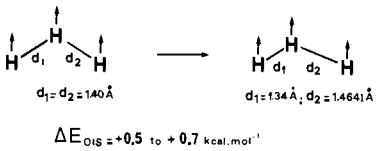

14

positive (0.5–0.7 kcal/mol) at the different computational levels.[42] This slight resistance to distortion originates in the overlap repulsion between the electrons that possess identical spins. Since the overlap between hydrogen orbitals is larger than the corresponding π-type overlap[43] in **13**, the π-contribution to the distortion energy in quadruplet allyl will be even smaller than 0.5–0.7 kcal/mol. A *lower* limit estimate of ΔE_{dis}^{σ} can be derived then by subtracting 0.5–0.7 kcal/mol from the total distortion energy of quadruplet allyl, **13**.

The so derived ΔE_{dis}^{σ} values are shown in Table II along with the total distortion energy, $\Delta E_{dis}^{\pi,\sigma}$, of the ground-state allyl radical. It is apparent that the *lower limit* ΔE_{dis}^{σ} values are slightly larger than the total distortion energy of the ground-state allyl radical at all the computational levels. Thus, very simple considerations already show that the delocalized π-component of the ground-state allyl radicai is either prone to or indifferent to a localizing distortion.

To reinforce the above conclusion, exact ΔE_{dis}^{σ} values must be derived. This can be achieved by partitioning the total SCF energy expression for quadruplet allyl radical into π- and σ-contributions as shown in eq 5.[44] Here h_π and h_σ are the corresponding mo-

$$E_{tot}^{\pi,\sigma} = \overset{occ}{\sum} h_\pi + R_{\pi\pi} + R_{\pi\sigma} + \overset{occ}{\sum} h_\sigma + R_{\sigma\sigma} + V_{NN} \tag{5}$$

noelectronic integrals of the π- and σ-spin –orbitals. The R terms stand for electron–electron repulsion of a type that is specified by the subscript, and V_{NN} accounts for nuclear repulsion. The last three terms describe the energy of the σ-framework, $(C^{1+})_3H_5$, with effective positive charges residing on the carbon atoms as shown in **15**. In turn, the first three terms in the equation describe the electronic energy of the quadruplet allyl in the field of the σ-framework **15**.

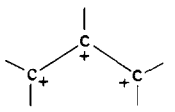

15

The σ–π partition described in eq 5 is routinely used in π-electron calculations.[45] However, in ab initio calculations V_{NN} cannot be partitioned into σ- and π-components, and it is precisely for circumventing this difficulty that the localizing distortions in Figure 2 are adapted so as to keep constant nuclear repulsion between carbons. In this manner, the π- and σ-contributions to $\Delta E_{dis}^{\pi,\sigma}$ of quadruplet allyl **13** can be identified with the corresponding *variations* in the π- and σ-electronic energies in eq 5.[44] Further accuracy of the π-contribution can be achieved by inclusion of π-space correlation (π-CI) which does not affect ΔE_{dis}^{σ}. In this manner one obtains ΔE_{dis}^{σ} values that represent the reluctance of the σ-frame to distort asymmetrically *in the field of nonresonating π-electrons*.

Another way to model the σ-frame is to calculate directly the σ-frame described in **15** in keeping with the definition in eq 5. Once obtained, the ΔE_{dis}^{σ} values are compared with the total distortion energies, $\Delta E_{dis}^{\pi,\sigma}$ of ground-state allyl radical, in order to ascertain the role of π-electronic delocalization more accurately than in Table II. The various ΔE_{dis} values, at different levels of

Table II. Comparison of Distortion Energies (kcal/mol), ΔE_{dis}^{σ} (Lower Limit) and $\Delta E_{dis}^{\pi,\sigma}$, for Allyl Radical

method	C_3H_5 (quadruplet) ΔE_{dis}^{σ} (lower limit)[b,c]	C_3H_5 (ground state) $(\Delta E_{dis}^{\pi,\sigma})^c$
STO-3G/π-CI[a]	+5.3	+2.5
6-31G/π-CI[a]	+4.4	+3.9
6-311G/π-CI	+4.3	+3.8
6-311G/(π + σ)-CI	+4.5	+4.4

[a] The CI is performed for the ground state. [b] These values are obtained by subtracting 0.7 (STO-3G level) and 0.5 kcal/mol (6-31G and 6-311G levels) from the total distortion energy of quadruplet allyl (see **14**). [c] $\Delta E_{dis} > 0$ means reluctance to distort.

Table III. Distortion Energies (kcal/mol)[a] for Allyl Radical at Different Computational Levels

species[d]	method	$\Delta E_{dis}^{\pi,\sigma}$	ΔE_{dis}^{σ}[b]	ΔE_{dis}^{π}
	(I) STO-3G			
(1) C_3H_5 (quadruplet), **13**	SCF	+6.0	+5.7	
(2) C_3H_5 (ground state), **12**	π-CI	+2.5	+5.7	-3.2
(3) $(C_3H_5)^{3+}$, **15**	SCF		+5.7	
	(II) 6-31G			
(4) C_3H_5 (quadruplet), **13**	SCF	+4.9	+4.8	
(5) C_3H_5 (ground state), **12**	π-CI	+3.9	+4.8	-0.9
(6) $(C_3H_5)^{3+}$, **15**	SCF		+4.8	
	(III) 6-311G			
(7a) C_3H_5 (quadruplet), **13**	SCF	+4.8	+4.7	
(7b) **13**	π-CI	+4.8	+4.7	
(7c) **13**	(π + σ)-CI	+5.0	+4.9	
(8a) C_3H_5 (ground state), **12**	π-CI	+3.8	+4.7	-0.9
(8b) **12**	(π + σ)-CI	+4.4	+4.9	-0.5

[a] $\Delta E_{dis} > 0$ means nondistortive species; $\Delta E_{dis} < 0$ means distortive species. [b] ΔE_{dis}^{σ} values are estimated by using eq 5 on the quadruplet allyl in **13**. [c] This ΔE_{dis}^{σ} value is obtained by subtracting 0.1 kcal/mol from the $\Delta E_{dis}^{\pi,\sigma}$ value, as in entry 7b. Using the method in ref 2a, one obtains the same value. [d] Entry numbers are in parentheses.

(42) The distortion energies of quadruplet H_3 are 0.74 kcal/mol at the STO-3G level and 0.48 kcal/mol at the level of 6-311G + CI. See ref 2a.

(43) H···H overlap is 0.296 while the π-type overlap is 0.213 at the STO-3G level, at the distance of 1.40 Å.

(44) The π-energy is obtained by summing up the energies of the occupied π-spin–orbitals and subtracting once the π electron–electron repulsion integrals, since these are counted twice in the summation.

(45) Bishop, D. M. *Group Theory and Chemistry*; Clarendon: Oxford, 1973; p 204.

Table IV. Distortion Energies (kcal/mol)[a] for Benzene at Different Computational Levels

species[d]	method	$\Delta E_{dis}^{\pi,\sigma}$	ΔE_{dis}^{σ} [b]	ΔE_{dis}^{π}
	(I) STO-3G			
(1a) C_6H_6 (ground state)[b]	SCF	+5.2	+17.1	−11.9
(1b) C_6H_6 (ground state)[b]	π-CI	+5.9	+17.1	−11.2
(2) $(C_6H_6)^{6+}$, **17**	SCF		+17.3	
(3) C_6H_6 (septuplet), **16**[c]	SCF	+18.1	+16.9	
	(II) 6-31G			
(4a) C_6H_6 (ground state)[b]	SCF	+6.6	+16.3	−9.7
(4b) C_6H_6 (ground state)[b]	π-CI	+7.2	+16.3	−9.1
(5) $(C_6H_6)^{6+}$, **17**	SCF		+14.1	
(6) C_6H_6 (septuplet), **16**[c]	SCF	+14.5	+13.7	

[a] $\Delta E_{dis} > 0$ means nondistortive species; $\Delta E_{dis} < 0$ means distortive species. [b] ΔE_{dis}^{σ} and ΔE_{dis}^{π} values are obtained by applying eq 5 to the ground state. [c] ΔE_{dis}^{σ} values are obtained by applying 5 to the septuplet state. [d] Entry numbers are in parentheses.

sophistication, are collected in Table III. The ΔE_{dis}^{σ} values are seen to converge as the level of sophistication increases (compare entries 4–7 in Table III), and the accuracy does not change when the basis set is elevated (to 6-311G) and σ-correlation is added. The value of $\Delta E_{dis}^{\sigma} = +4.8$ kcal/mol is not likely to change then upon further elevation of the computational level. Comparison of ΔE_{dis}^{σ} to $\Delta E_{dis}^{\pi,\sigma}$ of the ground-state allyl radical provides a clear-cut trend: the resistance of the species to distort is lowered when π-delocalization is present. The delocalized π-component of the ground state of allyl radical appears to be distortive and to prefer a localized electronic structure ($\Delta E_{dis}^{\pi} < 0$). At the highest computational level, which involves a triple-ζ basis set and extensive σ- and π-CI, the π-component of ground-state allyl radical is found to prefer a localized structure by 0.5 kcal/mol (entry 8b, Table III). Be it as it may, the driving force for the symmetric structure of ground-state allyl radical is provided entirely by the σ-framework, while the delocalized π-component is either indifferent to or slightly unstable toward a localizing distortion. It follows then that *π-electronic delocalization in allyl radical is a byproduct of the geometric constraint imposed by the σ-frame.* This conclusion confirms the predictions of the qualitative model[7] (section I) and is in harmony with recent VB calculations[30] and VB arguments.[8]

Benzene. The $\sigma-\pi$ partition for benzene is simpler than that for allyl radical, because unlike allyl radical[27] benzene does not exhibit Hartree–Fock instability. Due to this feature, ΔE_{dis}^{σ} and ΔE_{dis}^{π} can be estimated directly from the ground state of benzene by applying the $\sigma-\pi$ partition in eq 5. As before, π-CI will further improve the ΔE_{dis}^{π} values while not affecting the ΔE_{dis}^{σ} values.

For the sake of comparison, ΔE_{dis}^{σ} values are estimated also by the other two models used for allyl radical. In the first, π-delocalization is "turned off" in the π-septuplet state of benzene (**16**), and eq 5 is utilized to extract the ΔE_{dis}^{σ} value. In the second, ΔE_{dis}^{σ} is obtained by calculating the distortion energy of the bare σ-$(C^{1+})_6H_6$ framework (**17**).

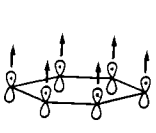

16

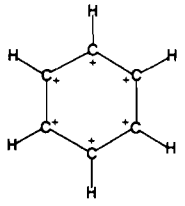

17

The various ΔE_{dis} values are summarized in Table IV at different computational levels. The small sensitivity of the results to the significant change in the computational level (entry 1a vs. 4b, Table IV) indicates that conclusions may be drawn with a wide margin of confidence.

Comparison of ΔE_{dis}^{σ} values to the $\Delta E_{dis}^{\pi,\sigma}$ values of the ground-state benzene projects clearly that the resistance of benzene to distort is lowered significantly (by >9 kcal/mol) when π-delocalization is present. The delocalized π-electrons of benzene unequivocally prefer a distorted and electronically localized structure ($\Delta E_{dis}^{\pi} < 0$ in entries 1 and 4). This distortive π-propensity is opposed by the stronger driving force of the σ-frame to maintain a uniform hexagonal structure ($\Delta E_{dis}^{\sigma} > 0$). The result is that electronic delocalization occurs in spite of the π-electrons and is a byproduct of the σ-imposed geometric constraint.

Comparing the π-distortive propensities (ΔE_{dis}^{π} values) of benzene and allyl radical, at the 6-31G/π-CI level, makes it apparent that the π-component of benzene is absolutely and relatively much more distortive than the π-component of allyl radical (Table IV entry 4b vs. Table III entry 5). This behavior is in exact analogy to the isoelectronic hydrogenic systems, where H_6 is at least 7-fold more distortive than H_3 (see Table I). This parallelism, as well as the computational results of the π-components, is in harmony with the predictions of the model in section I.

σ-Frames of C_3H_5 and C_6H_6. The ΔE_{dis}^{σ} values that can be compared are those that derive from the corresponding high-spin states, **13** and **16**, and the bare σ-frames, **15** and **17**. From Tables III and IV, the ratio $\Delta E_{dis}^{\sigma}(C_6H_6)/\Delta E_{dis}^{\sigma}(C_3H_5)$ is ~3 at the comparable computational levels. This value represents a physical picture of localized electron-pair σ_{CC}-bonds. In such a picture, the positive ΔE_{dis}^{σ} value derives from the reluctance of a couple of adjacent σ_{CC}-bonds to distort asymmetrically as shown schematically in **18**.[46] The total ΔE_{dis}^{σ} is proportional to the number of such adjacent couples of σ_{CC}-bonds. Since benzene possesses three such σ_{CC}-couples, while allyl only one, $\Delta E_{dis}^{\sigma}(C_6H_6)$ is 3-fold larger than $\Delta E_{dis}^{\sigma}(C_3H_5)$.

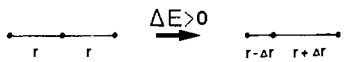

18

$\Delta E_{dis}^{\sigma}(C_6H_6)$ is estimated also directly from the ground state (entries 1 and 4 in Table IV). These $\Delta E_{dis}^{\sigma}(C_6H_6)$ values may be considered to represent more faithfully the σ-frame than the $\Delta E_{dis}^{\sigma}(C_6H_6)$ values that are obtained from the high-spin state (**16**) and the bare σ-frame (**17**). At the STO-3G level, all three $\Delta E_{dis}^{\sigma}(C_6H_6)$ values are practically equal. At the 6-31G level, however, the directly estimated value is 2.2–2.6 kcal/mol higher than the two other values (entry 4 vs. 5 and 6 in Table IV). This suggests that with extended basis sets, the bonding interactions of the π-electrons, as present in the ground state, tend to increase the ΔE_{dis}^{σ} value. One would expect to see the same σ-effect in allyl radical, but such a direct $\Delta E_{dis}^{\sigma}(C_3H_5)$ value cannot be estimated from the ground state. This direct value can, however, be evaluted from the ratio of the ΔE_{dis}^{σ} values discussed above, that is, $\Delta E_{dis}^{\sigma}(C_6H_6)/\Delta E_{dis}^{\sigma}(C_3H_5) = 3$.

Use of the extended basis set $\Delta E_{dis}^{\sigma}(C_6H_6)$ value, +16.3 kcal/mol, leads to $\Delta E_{dis}^{\sigma}(C_3H_5) = +5.4$ kcal/mol; a value which is 0.7–0.8 kcal/mol higher than the extended basis set values of $\Delta E_{dis}^{\sigma}(C_3H_5)$ in Table III. By use of the newly estimated $\Delta E_{dis}^{\sigma}(C_3H_5)$ value, in conjunction with the $\Delta E_{dis}^{\pi,\sigma}(C_3H_5)$ values of entries 4 and 8b of Table III, and improved $\Delta E_{dis}^{\pi}(C_3H_5)$ value of −1.1 to −1.3 kcal/mol can be obtained. Though this value of $\Delta E_{dis}^{\pi}(C_3H_5)$ is larger in absolute magnitude than the tabulated extended basis set $\Delta E_{dis}^{\pi}(C_3H_5)$ values, the thrust of the conclusion remains unaltered; the π-component of allyl radical is either indifferent to or slightly prone to distort, while the π-component of benzene strongly favors a distorted and localized structure.

Singlet Cyclobutadiene. It is well established that cyclobutadiene is rectangular.[39] The purpose of this section is to quantify the distortive π-propensity and to understand why the propensity is realized in cyclobutadiene but not in benzene.

The case of cyclobutadiene raises a particular difficulty in that different SCF theories must be used for the distorted and square structures. Indeed, while the distorted molecule has a closed-shell electronic structure and must be computed with a closed-shell type Fock operator (the classical Hartree–Fock theory), square cy-

(46) This result can be proved by using a simple harmonic potential for each σ-bond.

Table V. Distortion Energies (kcal/mol)[a] for Singlet Cyclobutadiene at Different Computational Levels

species[c]	method	$\Delta E^{\pi,\sigma}_{dis}$	ΔE^{σ}_{dis}	ΔE^{π}_{dis}
	(I) STO-3G			
(1) C_4H_4 (singlet)	π-CI[b]	−3.4	+10.3	−13.7
(2) $(C_4H_4)^{4+}$, **20**	SCF		+10.1	
(3) C_4H_4 (quintet), **19**	SCF	+10.2	+9.9	
	(II) 6-31G			
(4) C_4H_4 (singlet)	π-CI[b]	−3.4	+7.0	−10.4
(5) $(C_4H_4)^{4+}$, **20**	SCF		+7.8	
(6) C_4H_4 (quintet), **19**	SCF	+7.7	+7.6	

[a] $\Delta E_{dis} > 0$ means nondistortive species; $\Delta E < 0$ means distortive species. [b] The square cyclobutadiene is computed with the Davidson open-shell Hamiltonian and the distorted one with the closed-shell Hamiltonian. π-CI is then performed over the two species. [c] Entry numbers are in parentheses.

clobutadiene is a diradical with two degenerate singly occupied orbitals and is best computed within open-shell SCF theory.[35] Consequently, $\Delta E^{\pi,\sigma}_{dis}$ values are reliable only after subsequent π-CI on the square and the distorted structures. The σ-electrons are, in principle, treated equally by the two Hamiltonians so that the SCF level suffices to extract ΔE^{σ}_{dis} values. All the more, these ΔE^{σ}_{dis} values are in good agreement with the corresponding values obtained from the high-spin state, **19**, or the bare σ-frame, **20**, as shown in Table V.

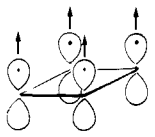

19

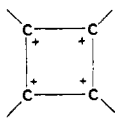

20

The $\Delta E^{\pi,\sigma}_{dis}$ and ΔE^{π}_{dis} values of C_4H_4 are, as expected, negative (entries 1 and 4 in Table V). What seems counter to previous conceptions is the fact that the ΔE^{π}_{dis} values are only slightly larger in absolute magnitude than the corresponding values for benzene. However, what should be compared in these two systems is the distortion energy per electron. Then it is seen that the π-component of C_4H_4 is significantly more distortive than that of C_6H_6, as expected on the basis of the concepts of aromaticity and antiaromaticity.

The σ-frame of C_4H_4 behaves approximately as one would expect by counting the number of adjacent pairs of σ_{CC}-bonds (two such pairs). In accord, $\Delta E^{\sigma}_{dis}(C_4H_4)$ is intermediate between $\Delta E^{\sigma}_{dis}(C_3H_5)$ and $\Delta E^{\sigma}_{dis}(C_6H_6)$. This intermediate $\Delta E^{\sigma}_{dis}(C_4H_4)$ value is insufficient now to constrain the "distortion-happy" π-electrons, and the species transforms to a rectangular structure.

Comparison of the π-Systems. It appears that the π-components of C_3H_5, C_4H_4, and C_6H_6 are all stabilized by a localizing distortion. In this sense, the π-components resemble qualitatively the corresponding H_n (n = 3, 4, 6)[4b,c] species that are all distortive regardless of any topological property (e.g., aromaticity). This distortive π-propensity is always opposed by the σ-frames which wish to maintain uniform structures with equal bond lengths. It follows then that the driving force for the uniform structures of allyl radical and benzene originates entirely in the σ-frame, and π-electronic delocalization is a byproduct of this σ-imposed geometric constraint. These conclusions are in full conformity with the qualitative analysis of the VB correlation diagram model (section I).

At this point one might wonder whether this π-propensity would persist if another $\sigma-\pi$ partition had been chosen. Although this partition is theoretically well founded and used in all π-electron theories, we have verified that the above tendencies are unchanged when $R_{\pi\sigma}$ integrals are equally shared among the π- and σ-systems rather than fully attributed to the π-system.

III. Distortive π-Propensities vs. Other Properties of π-Systems

The above conclusions raise some questions. How can the π-components of allyl radical and benzene possess distortive propensities when strong indications exist that these modes of π-delocalization are stabilizing? If the π-component of cyclobutadiene behaves qualitatively like the π-component of benzene, then where are the Hückel rules that are nevertheless so successful? What are the origins of the particular thermochemical stability of benzene[47,48] and the rotational barrier in allyl radical?[49] The following sections show that all these π-properties exist in harmony with the distortive π-propensity. To understand this, it is necessary to establish the relationship between three different concepts: the distortive propensity, the stabilization by delocalization, and the thermochemical properties.

Table VI. Quantum Mechanical Resonance Energies[a] (QMRE or B) for Hexagonal C_6H_6 and H_6 and Square Singlet C_4H_4

species[d]	QMRE (B)	QMRE per electron
	(I) STO-3G	
(1) C_6H_6 (hexagonal)	107.3	17.9
(2) H_6 (hexagonal)[b]	132.3	22.1
(3) C_4H_4 (square)[c]	45.2	11.3
	(II) 6-31G	
(4) C_6H_6 (hexagonal)	85.2	14.2
(5) H_6 (hexagonal)[b]	118.8	19.8
(6) C_4H_4 (square)[c]	30.2	7.6

[a] In kcal/mol. After ref 48 (see Appendix 2). [b] Optimized structure at the CI level. See ref 4d. [c] The localized Kekulé form is straightforwardly obtained from the closed-shell Hamiltonian. [d] Entry numbers are in parentheses.

1. Stabilization by Delocalization: Quantum Mechanical Resonance Energy (QMRE). What happens when it is possible to draw, in *a given geometry*, more than one Kekulé structure for an electronic system? For any given geometry, the wave function resulting from the variational mixing of these structures will be lower in energy than those of the pure Kekulé components. This is true in any case, be it aromatic, antiaromatic, or nonaromatic. Such stabilization corresponds to the term B in the VB correlation diagram of Figure 1 and had been called before by Coulson[50] "Quantum Mechanical Resonance Energy" (QMRE). The value of B or QMRE carries within it the topological information such as that associated with Hückel rules.

The QMRE can be computed by using the procedure developed by Kollmar.[48,51] In this procedure, QMRE is simply the ab initio SCF energy difference of the delocalized system and its localized Kekuléan structure at a given geometry, as shown schematically in **21** for benzene (see Appendix 2).

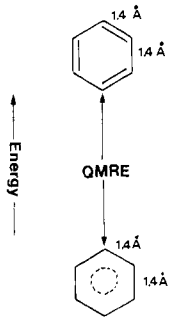

21

The so obtained QMRE values for benzene, square singlet cyclobutadiene, and hexagonal H_6 are collected in Table VI. It

(47) For some recent papers on the thermochemical stability of benzene and instability of cyclobutadiene, see: (a) Haddon, R. C. *J. Am. Chem. Soc.* **1979**, *101*, 1722. (b) Haddon, R. C.; Raghavachari, K. *J. Am. Chem. Soc.* **1985**, *107*, 28. (c) Hess, B. A.; Schaad, L. J. *J. Am. Chem. Soc.* **1983**, *105*, 7500.

(48) Kollmar, H. *J. Am. Chem. Soc.* **1979**, *101*, 4832.

(49) (a) Korth, H.-G.; Trill, H.; Sustmann, R. *J. Am. Chem. Soc.* **1981**, *103*, 4483. (b) Viehe, H. G.; Janouzek, Z.; Meenyi, R. *Acc. Chem. Res.* **1985**, *18*, 148.

(50) Coulson, C. A.; Altman, S. L. *Trans. Faraday Soc.* **1952**, *48*, 293.

(51) Daudey, J. P.; Trinquier, G.; Barthelat, J. C.; Malrieu, J. P. *Tetrahedron* **1980**, *36*, 3399.

is apparent that all the species, including cyclobutadiene, involve substantial QMRE. Further inspection projects two major conclusions. First: the Hückel rules which are *orbital* symmetry based are reflected by the QMRE values. Thus aromatic delocalization, like that in H_6 and in C_6H_6, is indeed favorable over delocalization of four electrons in C_4H_4. The computational results are then in harmony with previous views on electronic delocalization. It should be noted that the QMRE values reported here are estimated in the framework of SCF theory. Therefore, they take into account the resonance interaction between Kekulé structures but neglect the correlation energy of each bond and might slightly differ from the *B* values, as computed in the VB framework.

Second: QMRE is unrelated to the distortive property of the delocalized species. Thus, the most distortive species, H_6, possesses the largest QMRE. The QMRE simply reflects the potential of the system to enjoy stabilization by delocalization *at a given geometry*. However, this is not the only driving force in a distortive propensity *from this geometry*. Indeed, as projected from Figure 1, establishing the point of maximal delocalization involves an energy rise (reorganization energy), and then QMRE (*B*) is gained through delocalization. It is the balance between these factors that determines the distortive propensity. Thus large reorganization energy results in a distortive delocalized state, though this may be typified by QMRE (stabilization) at a given fixed geometry. The computed distortive propensities of the π-components in allyl radical and benzene are then in harmony with the fact that these two species enjoy substantial QMRE at their regular geometries. Different sets of experiments will be required to unravel these two different properties.

2. Relationship between Thermochemical Stability, QMRE, and Distortive Propensities. To demonstrate that there is no contradiction between the distortive π-propensities and the thermochemical properties of the target π-systems, it is necessary to present the computational results in a manner that reflects the harmony between the two properties.

Thermochemical Resonance Energy of C_6H_6. In terms of modern theories,[47,48,52] the thermochemical resonance energy (TRE) is defined as the energy difference between benzene and a reference molecule (R) that is a cyclic hexatriene having the same degree of interbond π-conjugation as in the open-chain polyene.[52] Since π-energies in polyenes are additive[47,48,52] the reference molecule is taken to be simply hexatriene that is, figuratively, tied unto itself to afford one additional π-conjugative interaction and one additional σ-bond, as shown in **22** where the dotted lines indicate π-conjugative interactions.

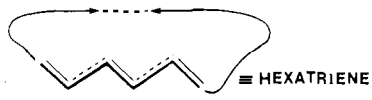

22 (R)

Kollmar has pointed out[48] that the TRE can be obtained from ab initio calculations by computing quantum mechanical resonance energies (QMRE) as discussed in section III.1 (see, for example, **21**). By use of Kollmar's method[48] the TRE of benzene can be calculated by using the thermochemical cycle in **23**. Here, the

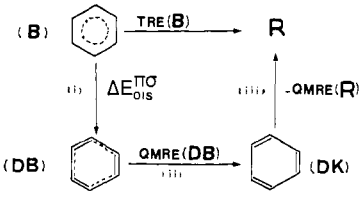

23

first step, i, involves distortion of benzene to yield distorted benzene (DB). The energy change involved in this process is the $\Delta E^{\pi,\sigma}_{dis}$ value that is shown in Table IV to involve a distortive π-component ($\Delta E^{\pi}_{dis} < 0$) and an opposing σ-component ($\Delta E^{\sigma}_{dis} > 0$). In the second step, ii, the residual π-conjugation of DB is turned off to afford the distorted Kekulé structure DK. The energy change in this process is the QMRE of distorted benzene, that is, QMRE(DB). The third step, iii, involves a partial restoration of the π-conjugation to the degree that is present in the reference cyclohexatriene molecule (R). The energy change in this process is the negative value of the QMRE of R, that is, -QMRE(R). The sum of these energy changes then yields the requested thermochemical resonance energy of benzene, TRE(B), as expressed by eq 6.

$$\mathrm{TRE(B)} \approx \Delta E^{\sigma}_{dis} + \Delta E^{\pi}_{dis} + \mathrm{QMRE(DB)} - \mathrm{QMRE(R)} \quad (6)$$

Kollmar has shown that the QMRE of polyenes is nearly additive:[48] it simply is the QMRE of butadiene multiplied by the number of interbond π-conjugative interactions. The reference molecule R in **22** involves three such π-interactions, and at the 6-31G level one obtains that QMRE(R) = 28.5 kcal/mol. At the same computational level QMRE(DB) is 53.5 kcal/mol. With the 6-31G values for ΔE^{π}_{dis} and ΔE^{σ}_{dis} from Table IV (entry 4a), TRE (B) comes out to be 31.6 kcal/mol. This value is very close to the one obtained by Kollmar[48] using another double-ζ basis set and a slightly different geometry for the distorted benzene (DB).

It is possible to give, now, a detailed partition of the TRE (B) value in terms of π- and σ-contributions. The total π-component in eq 6 is +15.3 kcal/mol. This value is the net effect of the π-distortive energy in benzene (ΔE^{π}_{dis} = -9.7 kcal/mol) and the QMRE difference between distorted benzene and the reference molecule R (ΔQMRE = +25.0 kcal/mol). This π-component is augmented by a σ-component (ΔE^{σ}_{dis}) of +16.3 kcal/mol that results from the reluctance of the σ-frame to distort from a symmetric hexagonal structure.

It follows from the above partition that there is no contradiction between the distortive π-propensity of benzene and its overall stability relative to some reference molecule. The π-contribution to this relative thermochemical stability originates in a better π-conjugation in benzene relative to the imaginary reference, R. Put differently, the net π-effect of TRE(B) measures a quantity that derives from the QMRE(C_6H_6) property that was discussed before (**21**, see also *B* in Figure 1). This property, as we have witnessed from Table VI, exists in harmony with another property, the π-distortive propensity.

Rotational Barrier in C_3H_5. By use of an analogous thermochemical cycle, it is possible to show how allyl radical exhibits a rotational barrier despite the distortive propensity of its π-component. This cycle is shown in **24** and involves and initial deformation to a distorted planar allyl (DA). The energy change

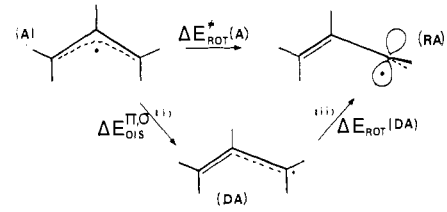

24

in this first process is the distortion energy, $\Delta E^{\pi,\sigma}_{dis}$. In the second process, DA undergoes a 90° rotation about its C=C bond and thereby loses its residual π-conjugation. This process involves an energy rise, ΔE_{rot}(DA), due to a loss of the QMRE of the distorted allyl. Once again then, the thermochemical observable ΔE^{*}_{rot}(A) is a sum of σ- and π-contributions. The fact that this observable is positive does not contradict the distortive propensity of the delocalized π-component of allyl radical.

A lower limit of the QMRE of distorted allyl, step ii, can be estimated from the known rotational barrier ($\sim$15 kcal/mol)[49] and the best $\Delta E^{\pi,\sigma}_{dis}$ value of +4.4 kcal/mol in Table III (entry 8b). The result of $\sim$10 kcal/mol constitutes a substantial fraction of the rotational barrier. To remind the reader, the QMRE is related to the avoided crossing resonance interaction in Figure 1. The

(52) The modern theories rely on the Dewar definition of TRE. See: (a) Dewar, M. J. S.; de Llano, C. *J. Am. Chem. Soc.* **1969**, *91*, 789. (b) Dewar, M. J. S.; Gleicher, G. J. *J. Am. Chem. Soc.* **1965**, *87*, 685, 692.

distorted allyl possesses a geometry that is very close to the geometry of the crossing point, and therefore the QMRE at the distorted geometry is a substantial part of the QMRE of symmetric allyl (*B* in Figure 1). Consequently, the rotational barrier experiment measures a property of allyl that is related to the QMRE at the crossing point.

Thermochemical Instability of C_4H_4. An analogous cycle to **23** is presented in **25** for C_4H_4. By use of the usual definition,[47,48,52] the reference molecule (R) is butadiene tied unto itself. However,

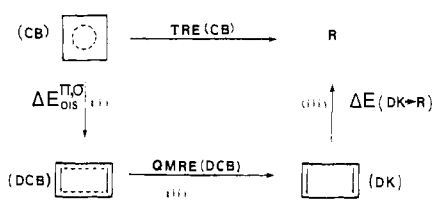

25

now the distorted Kekulē structure, DK, and the reference molecule, R, possess fundamentally different features, because the π-bonds in DK face one another, while in R they are mutually canted away. Therefore the ΔE(DK → R) term in step iii of **25** must take this difference into account.

A major effect caused by this difference is the π-overlap repulsion in DK relative to that in the Kekulē form of R. Since the two localized π-bonds in DK are forced face on, the resulting π-overlap repulsion is far greater than the corresponding factor in the Kekulē form of R. With Kollmar's method,[48] the *excess* π-overlap repulsion is estimated to be ~40 kcal/mol at the STO-3G level (see Appendix 2).

In step iii in **25**, this excess π-repulsive interaction is relaxed, and typical polyenic delocalization of R is established. Therefore, the energy change involved in this process (iii) is a large negative quantity. Similarly, $\Delta E_{dis}^{\pi,\sigma}$ in step i is also negative, while QMRE(DCB) in step ii is a small positive quantity (<20 kcal/mol at the 6-31G level).[53] Consequently, the thermochemical resonance energy of cyclobutadiene, TRE(CB), which is a sum of all the cycle's terms, turns out negative.

A negative TRE(CB) necessarily means thermochemical instability of C_4H_4 relative to the dienic reference R. Clearly then, the thermochemical instability of cyclobutadiene is not due to a lack of QMRE at the square geometry but rather to a high instability of the localized Kekulē form (DK in **25**).

The thermochemical properties of the three target molecules are found then to exist in harmony with the distortive propensities of their π-components. Experimental approaches other than thermochemistry or rotational barrier measurements will be required to probe the distortive propensities in C_6H_6 and in C_3H_5. Considerations of this type were offered by Berry,[24] long ago, from analysis of the vibrational spectrum of benzene. Designing new such experimental criteria is a challenge that if met will refine greatly the intimate knowledge of electronic structure.

Elusive N_6. It is instructive, before concluding, to project just how simple it is to apply the model to other conjugated systems. The elusive hexaazabenzene is a good example, owing to the many "whys" that surround this molecule.[10] Its elusiveness is not self-explanatory in view of the existence of C_6H_6. The molecule was computed by Saxe and Schaefer[10] and found to undergo a very facile B_{2u} deformation. Surprisingly enough, the N–N bond lengths were found to be very short. This—it was noted by Saxe and Schaefer[10]—might lead one to conclude that N_6 is even more aromatic than C_6H_6. These features require some simple explanations.

Our calculations show that at the 6-31G level, the π_{NN}-bond possesses a triplet excitation energy that is higher by ca. 15 kcal/mol than the corresponding value for π_{CC}. By utilization of the correlation diagram model, it is predicted that the π-component of N_6 will be more distortive than that of C_6H_6. Similarly, since the σ_{NN}-bond is much weaker than the σ_{CC}-bond,[14b,c] the σ-frame of N_6 is predicted to resist the localizing distortion to a lesser extent than the σ-C_6H_6 frame. The net ($\sigma + \pi$) outcome should then be an unstable N_6 species that easily distorts from D_{6h} symmetry.

Application of the σ–π partition method substantiates this straightforward prediction, as shown by the 6-31G/SCF distortion energies in **26**. Thus, for the same distortion (0.06 Å), the

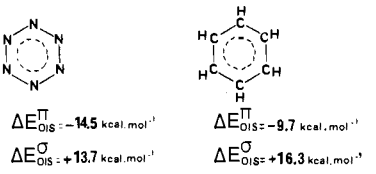

26

π-component of N_6 is substantially more distortive and is opposed by a weaker σ-driving force than in C_6H_6. This enhanced distortive character does not negate the possibility that the QMRE of N_6 may still be as large or even larger than that of C_6H_6. As we have shown, large QMRE and very strong distortive propensities can coexist in the same structure (e.g., H_6 in Table VI).

Analogous reasoning will show that electronic delocalization is seldom[7,8] going to be a driving force in conjugated systems composed of the second-row atoms C, N, and O. These compounds are just about the majority of delocalized species in organic chemistry.

IV. Concluding Remarks

The keynote of the paper is its leading question about the status of electronic delocalization in chemistry. In the perspective of the correlation diagram model (Figure 1), two opposite driving forces determine this status. Initially, reorganization energy is invested to force the Kekulē forms into resonance (the crossing point in Figure 1). Then, resonance interaction energy is gained by electronic delocalization (QMRE or *B* in Figure 1). The reorganization energy appears to dominate the trends of this opposition.[11]

For problems of neutral resonance the reorganization energy increases in proportion to the triplet excitation energy of the localized bond. Thus, *only atoms that form weak two-electron bonds, with low triplet excitation energy, can generate delocalized species that are stable toward a localizing distortion* (see **9a** vs. **9b**).

The results of the ab initio σ–π energy partition show that the π-components of the archetypal organic systems, benzene, allyl radical, and cyclobutadiene, abide by the above principle. Owing to the strength of the π_{CC}-bond, the π-components of these species are all distortive and resemble their corresponding isoelectronic H_n species. Electronic delocalization in C_3H_5 and C_6H_6 is then a *byproduct of the σ-imposed geometric constraint and not a driving force by itself.* Far from being a paradox, this finding unifies the delocalization problem and allows the π-components to fit neatly into a natural place in their respective isoelectronic series. Furthermore, harmony is shown to exist between the π-distortive propensities and other known thermochemical properties of the three organic species. Experimental deduction of the π-distortive propensities in C_3H_5 and C_6H_6 remains a challenging follow-up of this study.

Application of the correlation diagram model suggests that conjugated molecules involving third-row (or fourth-row, etc.) heteroatoms, such as silabenzene, silaallyl radical, and maybe even silacyclobutadiene, might possess nondistortive π-components.[7a] Studies of such species are under way.

Acknowledgment. The Centre Inter-Régional de Calcul Electronique (CIRCE) in Orsay is gratefully acknowledged for a generous allocation of computer time.

Appendix 1. Energy Gap (G) Expressions for X_3, X_4, and X_6

Consider the three-electron, three-center problem, X_3. The two Kekulē structures at their equilibrium geometries are shown in eq 1A, where a, b, and c are the atomic orbitals (or hybrids) of

(53) This is estimated as QMRE(DCB) = QMRE(CB) × [QMRE(DB)/QMRE(B)].

the X centers, in respective order.

$$\underset{K_1^0}{a\text{–}b} + c^\bullet \rightarrow \underset{K_2^0}{a^\bullet} + b\text{–}c \quad (1A)$$

From a computational point of view, K_1^* (Figure 1 of the text) is simply the bonding scheme of K_2^0 at the geometry that corresponds to K_1^0: with a···b being the short linkage and b···c being the infinitely long linkage. If we neglect AO overlap in the wave function, K_1^* becomes

$$K_1^* = \frac{1}{\sqrt{2}}[|ab\bar{c}| - |a\bar{b}c|] \quad (2A)$$

Similarly, neglect of overlap and ionic terms leads to K_1^0, whose wave function is given in eq 3A, where the a···b linkage is seen to involve singlet pairing. The energy of K_1^0 is that of a singlet a–b bond plus a radical, c (eq 4A).

$$K_1^0 = \frac{1}{\sqrt{2}}[|a\bar{b}c| - |\bar{a}bc|] \quad (3A)$$

$$E(K_1^0) = E_S(a\text{–}b) + E(c) \quad (4A)$$

In addition, there exists an excited state of K_1^0:

$$K_T^*(a\text{–}b) = \frac{1}{\sqrt{6}}[2|ab\bar{c}| - |a\bar{b}c| - |\bar{a}bc|] \quad (5A)$$

This state involves a pure triplet a···b linkage, and its energy is then simply

$$E(K_T^*) = E_T(a\text{–}b) + E(c) \quad (6A)$$

where $E_T(a\text{–}b)$ is the triplet energy of the a–b bond.

The wave function K_1^* can be reexpressed in terms of $K_T^*(a\text{–}b)$ and $K_1^0(a\text{–}b)$ to read

$$K_1^* = \frac{3}{\sqrt{2}}K_T^*(a\text{–}b) - \frac{1}{2}K_1^0 \quad (7A)$$

The corresponding energy then becomes

$$E(K_1^*) = {}^3/_4E_T(a\text{–}b) + {}^1/_4E_s(a\text{–}b) + E(c) \quad (8A)$$

The energy difference between K_1^* and K_1^0 is the gap of the diagram, G in Figure 1. The gap is then

$$G = E(K_1^*) - E(K_1^0) = {}^3/_4[E_T(a\text{–}b) - E_S(a\text{–}b)] = {}^3/_4\Delta E_{ST}(a\text{–}b) \quad (9A)$$

Let us now retain overlap and ionic terms. The corresponding K* wave functions do not involve ionic terms and read

$$K_1^* = \frac{1}{(2 - S^2)^{1/2}}[|ab\bar{c}| - |a\bar{b}c|] \quad (10A)$$

$$K_T^*(a\text{–}b) = \frac{1}{(6 - 6S^2)^{1/2}}[2|ab\bar{c}| - |\bar{a}bc| - |a\bar{b}c|] \quad (11A)$$

where S is the AO (hybrid) overlap of the a and b centers. The covalent definition of K_1^0 is similar

$$K_1^0(cov) = \frac{1}{(2 + 2S^2)^{1/2}}[|a\bar{b}c| - |\bar{a}bc|] \quad (12A)$$

Reexpressing K_1^* as done before leads to eq 13A. The corresponding energy of K_1^* becomes, accordingly, eq 14A, where

$$K_1^* = \frac{1}{2}\left(\frac{6 - 6S^2}{2 - S^2}\right)^{1/2}K_T^*(a\text{–}b) - \frac{1}{2}\left(\frac{2 + 2S^2}{2 - S^2}\right)^{1/2}K_1^0(cov) \quad (13A)$$

$$E(K_1^*) = \frac{3}{4}\left(\frac{2 - 2S^2}{2 - S^2}\right)E_T(a\text{–}b) + \frac{1}{4}\left(\frac{2 + 2S^2}{2 - S^2}\right)E_S^{cov}(a\text{–}b) + E(c) \quad (14A)$$

$E_S^{cov}(a\text{–}b)$ is the energy of a purely covalent a–b bond. The real a–b bond energy is lower than $E_S^{cov}(a\text{–}b)$ by a contribution, Δ_{ion}, that arises from the mixing of ionic terms $|a\bar{a}c|$ and $|b\bar{b}c|$ into K_1^0. The real singlet energy of a–b then becomes

$$E_S(a\text{–}b) = E_S^{cov}(a\text{–}b) - \Delta_{ion} \quad (15A)$$

Inserting eq 15A into eq 14A leads to

$$E(K_1^*) = \frac{3}{4}\left(\frac{2 - 2S^2}{2 - S^2}\right)E_T(a\text{–}b) + \frac{1}{4}\left(\frac{2 + 2S^2}{2 - S^2}\right)[E_S(a\text{–}b) + \Delta_{ion}] + E(c) \quad (16A)$$

The energy gap of the diagram then becomes

$$E(K_1^*) - E(K_1^0) = \frac{3}{4}\left(\frac{2 - 2S^2}{2 - S^2}\right)[E_T(a\text{–}b) - E_S(a\text{–}b)] + \frac{1}{4}\left(\frac{2 + 2S^2}{2 - S^2}\right)\Delta_{ion} \quad (17A)$$

that is

$$G = \frac{3}{4}\left(\frac{2 - 2S^2}{2 - S^2}\right)\Delta E_{ST}(a\text{–}b) + \frac{1}{4}\left(\frac{2 + 2S^2}{2 - S^2}\right)\Delta_{ion} \quad (18A)$$

From eq 18A one can see that inclusion of overlap tends to lower the gap below ${}^3/_4\Delta E_{ST}$, while inclusion of the ionic terms tends to raise the gap back to the limiting value of ${}^3/_4\Delta E_{ST}$. The net effect of including both ionic terms and overlap is that the diagram gap approaches the expression calculated by neglecting the two effects, as in eq 9A. The diagram gap can be approximately written then as eq 19A.

$$G \cong {}^3/_4\Delta E_{ST}(a\text{–}b) \quad (19A)$$

The case that will deviate the most from this expression is that of H_3. For this case the overlap term is quite large and the gap is about $0.6\Delta E_{ST}(H\text{–}H)$. This will not affect the trends because $\Delta E_{ST}(H\text{–}H)$ is so much larger than that of all other X–X bonds.

The above results show that neglect of overlap and ionic terms leads practically to the same gap expression as that obtained by retaining the two effects. Therefore, the X_4 and X_6 gaps are derived herein by neglecting overlap and ionic terms.

For any delocalization problem involving one electron per center the K_1^* and K_2^* wave functions in the diagram follow a simple structure. The long linkages are singlet paired, while the short linkages possess a mixture of singlet and triplet pairing, with the latter mode being dominant.

The energy of K_1^* is a normalized sum over the determinant's energies. Each determinant possesses an energy that is a sum of all the short linkages (infinite linkages possess zero energy). Consider a particular short linkage a···b. This linkage will have parallel spins in one-half of the determinants and antiparallel spins in the other half. For n such short linkages the energy of K_1^* then becomes

$$E(K_1^*) = n\left(\left\langle \frac{|a\bar{b}| + |ab|}{2^{1/2}}\middle|H\middle|\frac{|a\bar{b}| + |ab|}{2^{1/2}}\right\rangle\right) \quad (20A)$$

and in terms of state bond energies it reads

$$E(K_1^*) = n[{}^3/_4E_T(a\text{–}b) + {}^1/_4E_S(a\text{–}b)] \quad (21A)$$

The total energy of the ground state K_1^0 is simply the sum over the bonds of their singlet energies, that is

$$E(K_1^0) = nE_S(a\text{–}b) \quad (22A)$$

The diagram's gap is then given in eq 23A, where n is the number of localized bonds in a Kekulē structure. Thus, in each case of

$$G = E(K_1^*) - E(K_1^0) = n[{}^3/_4\Delta E_{ST}(a\text{–}b)] \quad (23A)$$

neutral delocalization the diagram's gap is proportional to the singlet to triplet excitation energy, and the proportionality is

determined by the number of localized bonds in a Kekulé structure.

Appendix 2. Ab Initio Determination of QMRE

This method was developed by Kollmar.[48] Using benzene as an example, one first performs a standard SCF calculation on benzene to obtain the SCF energy of the delocalized C_6H_6 species. In a second calculation, the pure Kekulé form is generated by replacing the delocalized π-MOs by three completely localized π-MOs extracted from a calculation of ethylene with the same C-C bond length as in benzene. The σ-MOs remain those of benzene. The three localized π-MOs are then orthonormalized by a unitary transformation which leaves the complete wave function unchanged. The SCF energy of this Kekulé form corresponds to a set of three localized π-bonds that interact by electron-electron and overlap repulsions. The SCF energy difference between the localized and delocalized C_6H_6 is then the requested QMRE as shown in **21** in the text.

Determination of Overlap Repulsion. The overlap repulsion can be estimated from the energy difference between two guess functions, one in which the localized ethylene π-bond orbitals are orthonormalized and one in which they are not. The energies of these two guess functions are obtained at the first cycle of the SCF calculation.

Registry No. $C_3H_5^{\bullet}$, 1981-80-2; C_4H_4, 1120-53-2; **2**, 71-43-2; N_6, 7616-35-5.

Mechanistics Studies on the Cobalt(II) Schiff Base Catalyzed Oxidation of Olefins by O_2

Dorothy E. Hamilton, Russell S. Drago,* and Alan Zombeck

Contribution from the Department of Chemistry, University of Florida, Gainesville, Florida 32611. *Received December 12, 1985*

Abstract: The cobalt complex [bis(salicylidene-γ-iminopropyl)methylamine]cobalt(II), CoSMDPT, has been shown to catalytically oxidize olefins in the presence of dioxygen or hydrogen peroxide. When terminal olefins are oxidized, the methyl ketone and corresponding secondary alcohol are produced selectively. Internal as well as terminal olefins are oxidized. The most common pathway for the oxidation of olefins catalyzed by first-row transition metals—autoxidation—has been ruled out in this system. A Wacker-type mechanism, oxidation by peracids, and mechanisms involving the formation of peroxymetallocycles have also been ruled out. A new mechanism for O_2 oxidations is proposed which involves oxidation of the primary alcohol solvent by CoSMDPT to produce the corresponding aldehyde and hydrogen peroxide. Reaction of hydrogen peroxide with CoSMDPT occurs to form a cobalt hydroperoxide, which can be viewed as a stabilized hydroperoxy radical which has spin paired with the d_{z^2} electron of CoSMDPT. The cobalt hydroperoxide then adds to the olefin double bond, leading to formation of an alkyl hydroperoxide. Haber-Weiss decomposition of this alkyl hydroperoxide by CoSMDPT produces the observed ketone and alcohol products. Deactivation of the catalyst is due to oxidation of the ligand system of the cobalt complex as well as formation of a μ-peroxo-dicobalt complex.

In almost all cases where selective catalytic oxidation of olefins is achieved, second- or third-row transition-metal complexes are involved, whereas first-row transition-metal complexes tend to be involved in autoxidation.[1-20] Autoxidation of olefins has been studied extensively over the past 40 years and is now generally recognized as a free-radical chain reaction. This chain reaction is often initiated by radical impurities or trace peroxides, which react with the olefins and generally form allylic radicals. The allylic hydroperoxide is formed and is decomposed to give products such as allylic ketones, allylic alcohols, epoxides, aldehydes, acids, and oligomers. Catalysts in autoxidation reactions are generally involved in either initiation of the chain reaction or in decomposition of the hydroperoxide intermediate. Because radical chain processes are involved, a mixture of products is often obtained.

Other reactions have been reported where oxidation of olefins occurs with remarkable selectivity, but second- or third-row transition-metal complexes are involved. These include Wacker-type processes, in which water is activated to transfer oxygen to the substrate,[7-11] and the oxidation of olefins by metal-nitro complexes,[12-16] which involves oxygen atom transfer from bound NO_2. Mimoun and others have also reported the selective oxidation of terminal olefins by rhodium complexes to form methyl

(1) Sheldon, R. A.; Kochi, J. K. *Metal-Catalyzed Oxidations of Organic Compounds*; Academic Press: New York, 1981; and references therein.
(2) Fuhrhop, J.-H.; Baccouche, M.; Penzlin, G. *J. Mol. Catal.* **1980**, *7*, 257.
(3) Dufour, M. N.; Crumbliss, A. L.; Johnston, G.; Gaudemer, A. *J. Mol. Catal.* **1980**, *7*, 277.
(4) Ohkatsu, Y.; Tsuruta, T. *Bull. Chem. Soc. Jpn.* **1978**, *51*, 188.
(5) Tetzuka, M.; Sekiguchi, O.; Ohkatsu, Y.; Osa, T. *Bull. Chem. Soc. Jpn.* **1976**, *49*, 2765.
(6) Kamiya, Y.; Beaton, S.; Lafortune, A.; Ingold, K. U. *Can. J. Chem.* **1963**, *41*, 2020.
(7) Smidt, J.; Hafner, W.; Jira, R.; Sedimeir, J.; Sieber, R.; Kojer, H. *Angew. Chem.* **1959**, *71*, 176.
(8) Smidt, J. *Chem. Ind. (London)* **1962**, 54.
(9) James, B. R.; Kastner, M. *Can. J. Chem.* **1972**, *50*, 1698.
(10) Osipov, A. M.; Matveev, K. I.; Shul'ts, N. N. *Russ. J. Inorg. Chem.* **1967**, *12*, 993.
(11) Bäckvall, J. E.; Åkermark, B.; Ljunggren, S. O. *J. Am. Chem. Soc.* **1979**, *101*, 2411.
(12) Tovrog, B. S.; Diamond, S. E.; Mares, F.; Szalkiewicz, A. *J. Am. Chem. Soc.* **1981**, *103*, 3522.
(13) Andrews, M. A.; Kelly, K. P. *J. Am. Chem. Soc.* **1981**, *103*, 2894.
(14) Diamond, S. E.; Mares, F.; Szalkiewicz, A.; Muccigrosso, D. A.; Solar, J. P. *J. Am. Chem. Soc.* **1982**, *104*, 4266.
(15) Andrews, M. A.; Cheng, C. A. *J. Am. Chem. Soc.* **1982**, *104*, 4268.
(16) Muccigrosso, D. A.; Mares, F.; Diamond, S. E.; Solar, J. P. *Inorg. Chem.* **1983**, *22*, 960.
(17) (a) Mimoun, H. *J. Org. Chem.* **1980**, *45*, 5387. (b) Igersheim, F.; Mimoun, H. *Nouv. J. Chim.* **1980**, *4*, 161. (c) Mimoun, H.; Perez-Machirant, M. M.; Seree de Roche, I. *J. Am. Chem. Soc.* **1978**, *100*, 5437.
(18) Farrar, J.; Holland, D.; Milner, D. J. *J. Chem. Soc., Dalton Trans.* **1975**, 815.
(19) Dudley, C. W.; Read, G.; Walker, P. J. *J. Chem. Soc., Dalton Trans.* **1974**, 1926.
(20) Drago, R. S.; Zuzich, A.; Nyberg, E. D. *J. Am. Chem. Soc.* **1985**, *107*, 2898.

0002-7863/87/1509-0374$01.50/0